THE TOTAL CAVOPULMONARY CONNECTION RESISTANCE: A SIGNIFICANT IMPACT ON SINGLE VENTRICLE HEMODYNAMICS AT REST AND EXERCISE

Kartik S. Sundareswaran[1], Kerem Pekkan[2], Lakshmi P. Dasi[1], Kevin Whitehead[3], Shiva Sharma[4], Kirk R. Kanter[5], Mark A. Fogel[3], Ajit P. Yoganathan[1]

[1]Wallace H. Coulter Department of Biomedical Engineering, Georgia Institute of Technology, Atlanta, GA

[2]Department of Biomedical Engineering, Carnegie Mellon University, Pittsburgh, PA

[3]Division of Cardiology, Children's Hospital of Philadelphia, Philadelphia, PA

[4]Pediatric Cardiology Services, Atlanta, GA

[5]Pediatric Cardiothoracic Surgery, Emory University School of Medicine, Atlanta, GA

Running Head: Impact of TCPC on hemodynamics

DISCLOSURES: NONE

Address correspondence to:

Ajit P. Yoganathan, Ph.D.

The Wallace H. Coulter Distinguished Faculty Chair in Biomedical Engineering and Regents Professor Associate Chair for Research

Wallace H. Coulter School of Biomedical Engineering

Georgia Institute of Technology and Emory University

Room 2119 U. A. Whitaker Building

313 Ferst Drive Atlanta, GA 30332-0535

TEL: 404-894-2849 FAX: 404-894-4243

Email: ajit.yoganathan@bme.gatech.edu

ABSTRACT

Introduction: Little is known about the impact of the total cavopulmonary connection (TCPC) on resting and exercise hemodynamics in a single ventricle (SV) circulation. The aim of this study was to elucidate this mechanism using a lumped parameter model of the SV circulation. ***Methods:*** Pulmonary vascular resistance (1.96 ± 0.80 WU) and systemic vascular resistances (18.4 ± 7.2 WU) were obtained from catheterization data on 40 patients with a TCPC. TCPC resistances (0.39 ± 0.26 WU) were established using computational fluid dynamic simulations conducted on anatomically accurate 3D models reconstructed from Magnetic Resonance Imaging (n=16). These parameters were used in a lumped parameter model of the SV circulation to investigate the impact of TCPC resistance on SV hemodynamics under resting and exercise conditions. A biventricular model was used for comparison. ***Results:*** For a biventricular circulation, the cardiac output (CO) dependence on TCPC resistance was negligible (sensitivity = -0.064 L/Min/WU), but not for the SV circulation (sensitivity = -0.88 L/Min/WU). Capacity to increase CO with heart rate was also severely reduced for the SV. At a simulated heart rate of 150 beats per minute, the SV patient with the highest resistance (1.08 WU) had a significantly lower increase in cardiac output (20.5%) when compared to an SV patient with the lowest resistance (50%) and the normal circulation (119%). This was due to the increased afterload (+35%) and decreased preload (-12%) associated with the SV circulation. ***Conclusion:*** TCPC resistance has a significant impact on the resting hemodynamics and exercise capacity of patients with an SV physiology.

Keywords: Mathematical Modeling, Cardiac Function, Congenital Heart Defects, Exercise, Magnetic Resonance Imaging

INTRODUCTION

The Fontan procedure comprising of connecting the systemic and pulmonary circulation in series via the total cavopulmonary connection (TCPC) is the primary palliative option for physiological correction of single ventricle (SV) congenital heart diseases[1, 2]. Although post operative survival is excellent, with some centers having a mortality of < 1%, studies have repeatedly demonstrated poor functional outcome in survivors[3-6], including - significantly reduced exercise capacity, diminished cardiac output, and risks of heart failure[4, 7-14]. Among all the parameters that come into play, decreased cardiac function in these patients seems to be one of the key players responsible for the poor functional outcome[12, 15]. However, the impact of the surgically altered TCPC on cardiac function or functional outcome has not been well understood.

Poor cardiac function in SV patients can be associated with many factors. For example, Fogel et al. demonstrated that the presence of the lateral tunnel baffle restricted the motion of the atrioventricular valve plane consequently resulting in increased afterload and decreased cardiac function[16]. Senzaki and colleagues argued that increased afterload, decreased preload (ventricular filling), and abnormal ventricular-vascular coupling are contributing factors for the decreased cardiac reserve and function in patients with a Fontan circulation[12]. A study by Szabo et al. reported increased afterload and decreased pre-load as well, using pressure-volume analysis conducted on measurements made in a dog single ventricle model[14]. Besides experimental studies, theoretical models have also predicted similar changes in afterload, preload, and cardiac reserve in a Fontan circulation[17-19].

Although these studies have demonstrated a strong link between cardiac function and functional outcome, the role of TCPC still remains unclear. As the TCPC surgical pathway

resistance is in series to the lungs, it has an effect similar to increasing the pulmonary vascular resistance (PVR) as pictured by Guyton's isolated venous theory[20-22]. According to Guyton, single ventricle cardiac output is highly sensitive to the PVR which is located downstream of the venous compliance. Recent experimental and computational studies have repeatedly demonstrated the elevated energy losses due to the highly complex nature of flow structures in the TCPC, which have a compounding effect on the overall resistance experienced by the venous system[23-26]. This hints that the TCPC resistance could play a big role in regulating cardiac output during resting and exercise conditions in Fontan patients.

In order to cope up with the increased resistance and maintain the desired cardiac output in the absence of a pulmonary ventricle, there is a significant drop in venous compliance of the Fontan physiology (-400%)[27]. Consequently, there is a ten-fold increase in central venous pressures (CVP). Such high CVP have been speculated to cause disorders associated with the hepatic system, such as protein-losing-enteropathy[28]. Therefore, it is critical to understand the quantitative relationship that exists between TCPC resistance and CVP as well so that treatment and management strategies can be designed not only for achieving good cardiac function, but also for the normal functioning of the hepatic system [29, 30].

These findings indicate that optimizing Fontan surgeries to reduce TCPC resistance could have an impact on cardiac and hepatic function, and as a result improve the functional outcome of SV patients. Therefore, the primary objective of this study is to quantify the impact of the resistance induced by the geometry of the TCPC on cardiac function and hemodynamics of the Fontan physiology both at rest and exercise. This hypothesis is tested using a lumped parameter single ventricle model, with parameters obtained from patient magnetic resonance imaging (MRI), and cardiac catheterization data.

METHODS

Patient Data

A multi-center Fontan patient cardiac MRI database of over 200 patients has been established to study the anatomic elements of the TCPC. The acquisitions consisted of a stack of axial anatomic images for reconstruction of geometry, and cine phase contrast MRI (PC MRI) acquisitions for flow quantification at the superior vena cava (SVC), inferior vena cava (IVC), left pulmonary artery (LPA), and right pulmonary artery (RPA). Informed consent was obtained and all associated studies were approved by the Internal Review Boards of the Children's Hospital of Philadelphia, the Children's Healthcare of Atlanta, and Georgia Institute of Technology.

The 3D anatomic and flow reconstructions of the TCPC were generated using techniques previously developed and validated[31]. From this database, 16 patient specific geometries (6 intra-atrial, 9 extra-cardiac, 1 IVC-main pulmonary artery) were selected for computational fluid dynamic (CFD) simulations. The selected geometries are depicted in Figure 1. Table 1 shows the clinical data associated with each model selected in the study as well as the resting cardiac outputs obtained from PC MRI. In addition, cardiac catheterization data was also available on 40 patients with a single ventricle physiology which were used for estimating the vascular parameters for the systemic and pulmonary circulations. Specifically, systemic vascular resistance (SVR) and PVR measurements were used in the mathematical model, while the pressure and flow measurements were used for validating the model.

Computational Fluid Dynamics Simulations

The 3D anatomical reconstructions were used for grid generation in which vessel volumes were divided into computational elements (meshes). The number of elements varied depending on geometry size and complexity, and ranged from 548,842 to 1,674,440 for the models studied. At each element, the governing Navier-Stokes conservation equations of mass and momentum for laminar fluid flow were solved using FLUENT (Fluent Inc, Lebanon, OH). All solutions were obtained using second order solvers assuming a Newtonian fluid with a density of 1060 kg/m3 and viscosity of 3.71e-3 N-s/m^2. The patient-specific TCPC CFD analysis methodology and the *in vitro* validations of these techniques have been described in earlier studies[23, 32, 25]. For each patient-geometry, blood flow was modeled at baseline steady-state flow conditions by setting SVC and IVC flows to values derived from PC MRI averaged over the cardiac cycle. Outflows were defined by pressure boundary conditions, with values tuned to obtain the desired pulmonary flow splits at the equal vascular lung resistance (EVLR) condition described previously[23]. In order to determine the resistance of the TCPC under exercise conditions, simulations were also conducted as 1 L/Min increases for younger patients (3-7 years), and 2x and 3x the resting flow rates for older patients (>7 years), with the only exception being M15.

TCPC Resistance Evaluation

The CFD simulations were used to provide the pressure (P) and flow (Q) measurements throughout the TCPC pathway. Using the measurements at the inlets (SVC and IVC) and the outlets (LPA and RPA), the control volume energy loss was computed according to the following equation:

$$\dot{E}_{Loss} = P_{SVC} * Q_{SVC} + P_{IVC} * Q_{IVC} - P_{LPA} * Q_{LPA} - P_{RPA} * Q_{RPA} \quad \textbf{\textit{Equation 1}}$$

An energy loss based pressure drop term was then evaluated to estimate the resistance of the TCPC as shown:

$$\Delta P_{TCPC} = \frac{\dot{E}_{Loss}}{Q_{SVC} + Q_{IVC}} \quad \textbf{\textit{Equation 2}}$$

$$R_{TCPC} = \frac{\Delta P_{TCPC}}{\frac{(Q_{SVC} + Q_{IVC})}{BSA}} \quad \textbf{\textit{Equation 3}}$$

Description of the Lumped Parameter Model

In this study, an electric-circuit analog of the cardiovascular system similar to the lumped parameter model (closed-loop) developed previously by Pekkan et al[19] was used. This model was based on an earlier scheme proposed by Peskin et al[33] for the whole cardiovascular system, and was adapted here to study the Fontan physiology. This is a fairly simple model of the circulatory system (compared to the more complex models proposed by Magosso[17] and Migliavacca[34]), and has been used extensively to study normal and diseased configurations[19, 33, 35, 36]. Figure 2 shows the mathematical model for both the normal and SV circulations used in this study. The vascular parameters were the same for both biventricular and univentricular physiologies except for the: a) presence of a TCPC, b) absence of right ventricle, c) venous compliance.

The arteries, veins, and heart chambers were treated as pure time-dependent compliance chambers with lumped capillary and valve resistances. For the normal circulation, there is a chamber each for the left heart, systemic arteries, systemic veins, right heart, pulmonary arteries, and pulmonary veins. For the Fontan circulation, the right heart is replaced by a chamber

representing the TCPC. Each of these chambers (except the heart and the TCPC) has a resistance and compliance component mimicking the arterial and venous vessels in the cardiovascular system. As explained previously, SVR and PVR values were obtained from clinical cardiac catheterization data. Systemic and pulmonary compliance reflect typical Fontan values and are outlined in Table 2[27, 34, 37, 38]. The TCPC was treated as a dynamic resistance that changes with cardiac output and is evaluated using CFD simulations described above.

The advantage of such a mathematical model is that additional chambers or shunts can be introduced into the system, which is an option particularly valuable in congenital heart defect research. The instantaneous flow and pressure from compartments "i" to "j" were then evaluated by solving the following set of differential equations:

$$Q_{ij} = (P_j - P_i) * \frac{1}{R_{ij}} * S_{ij} - \frac{L_{ij} Q_{ij}}{R_{ij}} * S_{ij}$$
$$\frac{d(C_i P_i)}{dt} = \sum_{j-1}^{N} j(Q_{ij} - Q_{ji}) \qquad \textbf{\textit{Equation 4}}$$

Here the subscript "ij" depicts the flow from compartment "i" to compartment "j", where j is a compartment following "i". P_i and Qi, are the pressures and flows in chamber "i", R_{ij}, L_{ij}, and S_{ij} are the resistances, inertial effects of frictional forces, and switches enforcing the directionality of flows respectively. The magnitude of the inertial frictional effects on the fluid per unit cross-sectional area was estimated from $L_{ij}=4\rho l/(\pi D)^2$ and is introduced in Equation 4 as a lumped impedance for each compliant chamber. Vascular resistance values were obtained from cardiac catheterization, and compliance values were obtained from literature. The differential equation was solved iteratively for each chamber until the results converged.

The atria and ventricles themselves were modeled as time varying compliance chambers generating activation energies similar to those described by Sun et al[36]. Pulsatile pressure was generated in these models via functions that alternate between systolic (stiff) and diastolic (relaxed) ventricular activation functions. These activation functions govern the systolic and diastolic contraction properties of the myocardial muscle. The compliances were then used along with Equation 4 for generating the pressure waveforms within the 4 chambers of the heart respectively. Shown below are the equations used for generating the compliances:

$$E(t) = \frac{1 - e^{-t/T_C}}{1 - e^{-Ts/Tc}} \qquad 0 \le t \le Ts$$
$$CV(t) = CVD * (CVS / CVD)^{E(t)}$$
$$E(t) = \frac{1 - e^{-(t-Ts)/T_r}}{1 - e^{-(T-Ts)/T_r}} \qquad Ts \le t \le T \qquad \textbf{Equation 5}$$
$$CV(t) = CVS * (CVD / CVS)^{E(t)}$$

Tc (0.0025 minutes) and Tr (0.0075 minutes) are time constants governing the contraction and relaxation of the myocardial muscle during systole and diastole. T is the duration of one cardiac cycle (1/Heart Rate), Ts is the length of systole (T/3 at rest, T/2 at exercise), and t is the current point in the cardiac cycle. Systole and diastole were switched for modeling atrial contraction. CVD and CVS were the minimum and maximum compliance values of the chamber. The valves were modeled as linear unidirectional resistors with a resistance of 0.01 WU. Please note that 1 WU is equivalent to 1 mmHg/(L/Min) and is a commonly used clinical parameter to describe resistance to blood flow. The parameter values used in Equation 5 for each heart chamber are shown in Table 3.

Modeling Rest / Exercise Conditions and Data Analysis

Rest: To simulate the impact of TCPC resistance on cardiac output, R_{TCPC} in the model was uniformly varied from 0 WU to 1.8 WU (0 to 90% PVR) and its corresponding effect on cardiac output for the biventricular and univentricular circulations were evaluated. The range of TCPC resistances were selected based on computational models described above and were used to evaluate the sensitivity of the model to the TCPC resistance. For a biventricular circulation, since there is no TCPC, the pulmonary vascular resistance was increased by an equivalent amount. In addition, pressure volume analysis was conducted for a normal subject and TCPC cases with the highest, mean, and lowest resistances to demonstrate how the operating point of the univentricular circulation changes with resistance.

Exercise Conditions: In order to isolate the impact of just the TCPC resistance, the following parameters were changed for simulating exercise conditions:

1.) The heart rate was uniformly increased from 70 to 150 beats per minute simulating the primary response to exercise as outlined by several human and animal studies[7, 9-15, 17, 18, 39-42]. For the normal circulation, the ventricular contraction properties (CVD and CVS) were changed in addition to heart rate to model the typical response to exercise for a normal heart. This was not done for the SV circulation, as it has been previously demonstrated that Fontan patients increase CO primarily by increasing their heart rate, and do not change their ventricular contraction properties to increase stroke volume [12-14]. Therefore, only the heart rate was increased in the SV circulation as the primary response to exercise.

2.) SVR typically goes down with exercise demonstrating the impact of the peripheral muscular dynamics and the vasodilation that occurs to aid the increase in cardiac output[43]. Studies have shown a drop of almost 50% in SVR. This is accomplished in the model by decreasing the SVRI progressively from 18.5 WU as measured from catheterization data to 11 WU for both the normal and the SV circulation.

3.) There is also a significant impact of the pulmonary system and the lungs during exercise, especially in Fontan patients, where the negative intra-thoracic pressure greatly augments flow. Studies have reported a 40% drop in the PVR as a result of this phenomenon in addition to the local vasodilation that occurs to improve exercise tolerance[43]. Therefore the PVR in our model was gradually dropped from 1.96 WU as measured from catheterization to 1.1 WU based on the severity of exercise.

4.) As the cardiac output increases with increasing heart rate, so does the resistance of the TCPC. Figure 3 shows the dynamic range of TCPC resistances and how they change between the different geometries. As can be observed there is a non-linear increase in resistance with cardiac output. This phenomenon becomes important during elevated cardiac output conditions. To take this characteristic into account, the resistance of the TCPC (R_{TCPC}) was treated as a dynamic element that increased with an increase in cardiac output. TCPC resistance curves shown in Figure 3, were used for evaluating the correct resistance for each exercise condition.

Based on these exercise conditions, the following parameters were evaluated as a function of heart rate for the normal and SV circulations respectively: cardiac output (CO), end systolic pressure (ESP), central venous pressure (CVP), afterload (Ea), preload (Ees), ventricular-vascular coupling ratio (Ea/Ees), R_{TCPC}, and ratio of R_{TCPC} to pulmonary vascular resistance

(R_{TCPC}/R_{PVR}). Pressure volume loops were used to evaluate the slope of the end-systolic volume elastance or preload (Ees) and the vascular afterloading (Ea) property. These parameters were evaluated based on the methodology outlined by Senzaki[12], Szabo[14], and Nogaki[18]. The authors had full access to the data and take responsibility for its integrity. All authors have read and agree to the manuscript as written.

RESULTS

Single Ventricle Resistance

The average age and body surface area of the patients used in this study were 8.25 ± 4.28 (min= 2, max= 18) years, and 0.97 ± 0.28 (min=0.54, max=1.49) m^2 respectively. The measured PVR and SVR were 1.96 ± 0.80 (min = 1, max = 4.3) WU, and 18.4 ± 7.2 (min= 10.6, max= 47.8) WU respectively. Figure 3 shows the change in TCPC resistance with exercise for the models used in the study. TCPC resistances were 0.39 ± 0.26 WU (min=0.1, max=1.08) during rest, 0.70 ± 0.45 (min=0.13, max=1.72) during moderate exercise, and 1.06 ± 0.73 (min=0.18, max= 2.65) WU under severe exercise. The most efficient TCPCs at rest and exercise were M7 M9 respectively. The least efficient TCPCs at rest and exercise were M13 and M17. TCPC resistances were evaluated to be significant percentages of the measured PVR (22%) at rest).

Lumped Parameter Model

Figure 4 shows the pressure and flow waveforms in the aorta and pulmonary artery for a simulated resting heart rate of 70 BPM, and an average TCPC resistance of 0.39 WU. Systolic/diastolic aortic pressures were 117/85 mmHg and 115/73 mmHg for the normal and SV cases respectively. The lower diastolic pressures resulted in a lower mean aortic pressure of 95 mmHg (compared to 103 mmHg) for the single ventricle circulation. Cardiac output was

significantly lower for the SV circulation at 3.8 L/Min compared to 5.1 L/Min for the normal circulation. This can be attributed to the increased afterload experienced by the single ventricle due the lack of a pumping chamber on the right side. Pulmonary artery pressures were non-pulsatile in the single ventricle circulation that resulted in non-pulsatile flow in the pulmonary arteries, which was in corroboration with previous clinical studies. Table 4 shows a comparison of the modeled hemodynamic data vs. observed data from cardiac catheterization performed on 40 patients with a single ventricle physiology. There was a good match between what was predicted by the model and what was observed clinically demonstrating the validity of the model used for this study.

Effect of TCPC Resistance at Rest

Figure 5 shows the impact of TCPC resistance on hemodynamics in a SV and a normal circulation at a resting heart rate of 70 beats per minute (BPM). There is a drop in cardiac output going from a biventricular to a univentricular circulation at zero resistance, which is due to the lack of a systemic ventricle and the serial configuration of the two circulations. The sensitivity of cardiac output to the resistance of the TCPC in single ventricles was -0.88, which was significantly higher compared to -0.064 for the normal biventricular circulation. This implies that for every 10% increase in resistance, there is an 8.8% drop in cardiac output. Figure 5c shows the impact of TCPC resistance on CVP. The sensitivity of CVP to increase in the resistance of the TCPC was 0.64 implying that a 10% increase in resistance results in a 6.4% increase in CVP. The increase in CVP in single ventricles has been shown before using acute *in vivo* animal experiments[14], human studies[12], and theoretical studies[17, 18]. However, the impact of the TCPC procedure on CVP has been shown for the first time in this study. Figure 5b, 5d, 5e, and 5f show the effect of TCPC resistance on ESP, afterload, preload, and ventricular vascular coupling ratio

respectively. ESP increased, afterload increased, preload decreased, and ventricular vascular coupling ratio increased with increasing TCPC resistances respectively. Figure 6 shows the pressure volume loops associated with the normal and single ventricle circulations at rest and exercise. The area within the pressure volume loop signifies the net work done by the heart, which drops with increasing TCPC resistance demonstrating the improvement in ventricular work that can be accomplished by designing low resistance TCPCs.

Effect of TCPC Resistance during Exercise

Figure 7 depicts the hemodynamic responses to exercise as predicted by the model. The biventricular circulation was able to increase the cardiac output of 5.2 L/Min at 70 BPM to 11.4 L/Min at an exercise heart rate of 150 BPM (Figure 7a). This ability to increase CO was blunted in the SV circulation. In the SV, the increase in CO was only from 3.8 L/Min to 5.4 L/Min for a mean TCPC resistance of 0.39 WU; 4.4 L/Min to 6.8 L/Min for the TCPC with a minimum resistance of 0.1 WU; and 3.3 L/Min to 4.1 L/Min for a highly dissipative TCPC with a resistance of 1.08 WU.

The ESP of the ventricle also decreased progressively for the univentricular circulation, while there was a moderate increase in the biventricular circulation (Figure 7b). ESP at both rest and exercise was significantly lower for the case with the higher TCPC resistance. The increase in CVP was insignificant for the univentricular circulation and the biventricular circulation, an observation which was consistent with human measurements[12] (Figure 7c). The CVP was consistently higher for the TCPC with high resistance.

The afterload (Ea) experienced by the SV significantly increased with exercise compared to the biventricular circulation (Figure 7d). The presence of a highly dissipative TCPC further

increased the afterload. The increases were from 1.65, 1.62, and 1.7 to 2.23, 2.14, and 2.54 mmHg/mL for mean, minimum, and maximum R_{TCPC} values respectively. Although similar at rest, the differences increased with exercise. In comparison, the afterload only increased from 1.46 to 1.87 mmHg/mL for the biventricular circulation. Ventricular preload (Ees) increased (3.63 to 4.39 mmHg/mL) in the normal circulation, while it decreased in the case of the SV circulation (Figure 7e). For the three SV scenarios, Ees dropped from 3.12, 3.40 and 2.79, to 2.73, 3.24, and 2.26 mmHg/mL for mean, minimum, and maximum R_{TCPC} values respectively. This resulted in a mismatch in the preload and afterload experienced by the ventricle, resulting in an abnormal increase in the ventricular vascular coupling ratio (Ea/Ees) for the univentricular circulation, which was further worsened by the presence of a high resistance TCPC. While the Ea/Ees almost remained flat for a biventricular circulation, it increased for the univentricular circulation (7f). The increases were from 0.53, 0.48, and 0.61, to 0.82, 0.66, and 1.05 for mean, minimum, and maximum R_{TCPC} values respectively.

Finally, human studies have established that the PVR and the SVR go down with exercise[43]. However, the TCPC resistance increases with exercise as shown in Figure 3 implying that the TCPC bottleneck becomes more significant during exercise. Figures 7g and 7h, demonstrate that although at rest the TCPC resistance is a fraction of the pulmonary resistance (22%), this fraction significantly increases with exercise (50%). In fact, for the TCPC with a high resistance, this fraction increased from 55% at rest to 155 % during exercise, while for a low resistance TCPC this change was minimal going from 7% to 16%. This demonstrates the significant improvement that can be accomplished by optimizing the TCPC geometry.

DISCUSSION

Although the clinical prognosis of the Fontan procedure has significantly improved, the long term functional outcome is still subnormal, with a significant number of these patients demonstrating poor functional outcome and diminished exercise capacity[3]. Several studies have attributed this to the connection of the systemic and pulmonary circulation in series resulting in the increased afterload experienced by the single ventricle[12-14, 18, 40, 41]. However, all of these studies have not taken into account, the role of the TCPC geometry and the added resistance it imposes on the resting and exercise hemodynamics of the entire cardiovascular system. This study shows for the first time, utilizing mathematical modeling with patient-specific imaging, flow simulations, and cardiac catheterization measurements, the important role played by the surgically altered TCPC geometry on the overall resting and exercise hemodynamic capacity of patients with a Fontan physiology.

The significant variability of Fontan geometries translated to significant variability in resistances. The resistance of the "worst" TCPC was 10 times higher than the resistance of the "best" TCPC. This suggests that the TCPC procedures performed today are far from optimal, and more emphasis need to be given for optimizing the geometries pre-operatively. Especially, since the sensitivity of the univentricular circulation to changes in resistance is quite significant with a 10% increase in resistance resulting in an 8.8% decrease in cardiac output. To verify if this phenomenon is observed *in vivo*, cardiac index measured using PC MRI was plotted against the resistance evaluated using CFD for all the patients used in this study (Figure 8). Clearly a weak, but significant ($p < 0.05$) negative correlation can be observed between the TCPC resistance and the resting cardiac index measured on these patients. The slope of the correlation in the measurements is smaller compared to the one predicted by the model, which can be attributed to

the confounding factors associated with patient variability as well as the simplicity of the mathematical model used in this study.

The reduced capacity to increase cardiac output with exercise in single ventricle circulations has been well documented in the literature[3, 5, 7, 40]. However, the exact quantitative relationship between TCPC resistance and exercise capacity has been unclear, primarily because of two reasons: 1) lack of appropriate methods for quantifying TCPC efficiency, 2) complex interrelationships that exist between the respiratory, skeletal, and the cardiovascular system that make it difficult to establish correlations between the TCPC and exercise capacity. Therefore, there is a tendency to discount the impact of the TCPC on exercise as negligible. To address these issues, a thoroughly validated computational methodology was developed allowing for precise quantification of the TCPC resistance. Using these parameters in a lumped parameter model, demonstrated that the TCPC resistance does impair the ability of a SV to increase cardiac output with increasing demand. Although PVR drops as a result of exercise, the increased resistance of the TCPC with increasing cardiac output makes it the primary bottleneck during increased cardiovascular demand.

Figure 6 shows the pressure volume loops at rest for a normal biventricular circulation, and three single ventricle scenarios with ideal (zero) resistance, minimum, and maximum resistances respectively. Qualitatively these P-V loops match those observed in humans[12] and animals[14]. The reduced area under the P-V loop is a consequence of the Fontan physiology having both the systemic and pulmonary circulation in series. It is interesting to note that the reduction in area is more pronounced for the case of the TCPC with the highest resistance. The reduction area implies a reduction in the total power and reserve function available to the SV physiology during exercise further demonstrating the impact the TCPC can have on exercise capacity.

Clinically, it is observed that a majority of patients with a Fontan physiology have to take afterload reducing drugs as a result of the univentricular circulation[44]. This study demonstrates that more efficient TCPCs have the potential to reduce afterload, and hence lower the amount of medications prescribed to these patients. In addition, optimal TCPC geometries have improved flow dynamics in the baffle that may reduce the risk of thromboembolic complications. Therefore, geometric optimization of the TCPC could significantly benefit the univentricular circulation and more surgical emphasis should be laid on accomplishing this pre-operatively on a patient-specific basis. Previous studies on surgical planning and TCPC geometric optimizations have shown that significant improvements with reductions of over 50% in energy losses can be accomplished[45-50]. If appropriate surgical planning strategies are used then every patient-specific TCPC should have the lowest possible resistance given the anatomic constraints.

Although our model has a sound basis on clinically measured data and compares well with other clinical studies, the inherent limitations of this work are well acknowledged. Primarily, the resting and exercise hemodynamic conditions are modeled and are not empirically observed data. Specifically, the biochemical response to exercise, cardiopulmonary interactions, baroreflex response have not been modeled, in order to achieve a simpler model with less variables. Incorporating these responses will no doubt improve the accuracy of the model's predictions, however the relative impact of the TCPC resistance as illustrated here is not expected to change.

CONCLUSIONS

This is the first time the impact of TCPC surgical resistance on the overall hemodynamics of the univentricular circulation has been demonstrated. TCPC resistance has a direct impact on the afterload and the preload of the univentricular circulation and significantly impacts the resting

and exercise hemodynamics. The inability to increase cardiac output with exercise limits their ability to exercise and hence worsens their overall functional outcome. This can be countered by optimizing the geometry of the TCPC prior to the Fontan surgery that may result in decreased afterload and consequently an improvement in cardiac function.

ACKNOWLEDGEMENTS

This study was funded by a National Heart, Lung, and Blood Insitutes's Grant HL67622 and an American Heart Association's predoctoral fellowship award. We also acknowledge Dr W.James Parks from Children's Healthcare of Atlanta for providing data.

REFERENCES

1. de Leval MR. The Fontan circulation: What have we learned? What to expect? Pediatr Cardiol 1998;19(4):316-20.
2. de Leval MR, Kilner P, Gewillig M, Bull C. Total cavopulmonary connection: a logical alternative to atriopulmonary connection for complex Fontan operations. Experimental studies and early clinical experience. J Thorac Cardiovasc Surg 1988;96(5):682-95.
3. Marino BS. Outcomes after the Fontan procedure. Curr Opin Pediatr 2002;14(5):620-6.
4. Matthews IL, Fredriksen PM, Bjornstad PG, Thaulow E, Gronn M. Reduced pulmonary function in children with the Fontan circulation affects their exercise capacity. Cardiol Young 2006;16(3):261-7.
5. McCrindle BW, Williams RV, Mital S, Clark BJ, Russell JL, Klein G, et al. Physical activity levels in children and adolescents are reduced after the Fontan procedure, independent of exercise capacity, and are associated with lower perceived general health. Arch Dis Child 2007;92(6):509-14.

6. McCrindle BW, Williams RV, Mitchell PD, Hsu DT, Paridon SM, Atz AM, et al. Relationship of patient and medical characteristics to health status in children and adolescents after the Fontan procedure. Circulation 2006;113(8):1123-9.
7. Durongpisitkul K, Driscoll DJ, Mahoney DW, Wollan PC, Mottram CD, Puga FJ, et al. Cardiorespiratory response to exercise after modified Fontan operation: determinants of performance. J Am Coll Cardiol 1997;29(4):785-90.
8. Fredriksen PM, Therrien J, Veldtman G, Warsi MA, Liu P, Siu S, et al. Lung function and aerobic capacity in adult patients following modified Fontan procedure. Heart 2001;85(3):295-9.
9. Hjortdal VE, Emmertsen K, Stenbog E, Frund T, Schmidt MR, Kromann O, et al. Effects of exercise and respiration on blood flow in total cavopulmonary connection: a real-time magnetic resonance flow study. Circulation 2003;108(10):1227-31.
10. Joshi VM, Carey A, Simpson P, Paridon SM. Exercise performance following repair of hypoplastic left heart syndrome: A comparison with other types of Fontan patients. Pediatr Cardiol 1997;18(5):357-60.
11. Reybrouck T, Mertens L. Physical performance and physical activity in grown-up congenital heart disease. Eur J Cardiovasc Prev Rehabil 2005;12(5):498-502.
12. Senzaki H, Masutani S, Ishido H, Taketazu M, Kobayashi T, Sasaki N, et al. Cardiac rest and reserve function in patients with Fontan circulation. J Am Coll Cardiol 2006;47(12):2528-35.
13. Senzaki H, Masutani S, Kobayashi J, Kobayashi T, Sasaki N, Asano H, et al. Ventricular afterload and ventricular work in fontan circulation: comparison with normal two-

ventricle circulation and single-ventricle circulation with blalock-taussig shunts. Circulation 2002;105(24):2885-92.

14. Szabo G, Buhmann V, Graf A, Melnitschuk S, Bahrle S, Vahl CF, et al. Ventricular energetics after the Fontan operation: contractility-afterload mismatch. J Thorac Cardiovasc Surg 2003;125(5):1061-9.

15. Pedersen EM, Stenbog EV, Frund T, Houlind K, Kromann O, Sorensen KE, et al. Flow during exercise in the total cavopulmonary connection measured by magnetic resonance velocity mapping. Heart 2002;87(6):554-8.

16. Fogel MA, Weinberg PM, Fellows KE, Hoffman EA. Magnetic resonance imaging of constant total heart volume and center of mass in patients with functional single ventricle before and after staged Fontan procedure. Am J Cardiol 1993;72(18):1435-43.

17. Magosso E, Cavalcanti S, Ursino M. Theoretical analysis of rest and exercise hemodynamics in patients with total cavopulmonary connection. Am J Physiol Heart Circ Physiol 2002;282(3):H1018-34.

18. Nogaki M, Senzaki H, Masutani S, Kobayashi J, Kobayashi T, Sasaki N, et al. Ventricular energetics in Fontan circulation: evaluation with a theoretical model. Pediatr Int 2000;42(6):651-7.

19. Pekkan K, Frakes D, De Zelicourt D, Lucas CW, Parks WJ, Yoganathan AP. Coupling pediatric ventricle assist devices to the Fontan circulation: simulations with a lumped-parameter model. ASAIO J 2005;51(5):618-28.

20. Guyton AC. Cardiac Output, Venous Return, and Their Regulation: Saundersm Philadelphia, PA; 1961.

21. Guyton AC, Abernathy B, Langston JB, Kaufmann BN, Fairchild HM. Relative importance of venous and arterial resistances in controlling venous return and cardiac output. Am J Physiol 1959;196(5):1008-14.

22. Guyton AC, Lindsey AW, Kaufmann BN. Effect of mean circulatory filling pressure and other peripheral circulatory factors on cardiac output. Am J Physiol 1955;180(3):463-8.

23. Pekkan K, de Zelicourt D, Ge L, Sotiropoulos F, Frakes D, Fogel MA, et al. Physics-driven CFD modeling of complex anatomical cardiovascular flows-a TCPC case study. Ann Biomed Eng 2005;33(3):284-300.

24. Wang C, Pekkan K, de Zelicourt D, Horner M, Parihar A, Kulkarni A, et al. Progress in the CFD modeling of flow instabilities in anatomical total cavopulmonary connections. Ann Biomed Eng 2007;35(11):1840-56.

25. Whitehead KK, Pekkan K, Kitajima HD, Paridon SM, Yoganathan AP, Fogel MA. Nonlinear power loss during exercise in single-ventricle patients after the Fontan: insights from computational fluid dynamics. Circulation 2007;116(11 Suppl):I165-71.

26. Murakami H, Yoshimura N, Kitahara J, Otaka S, Ichida F, Misaki T. Collision of the caval flows caused early failure of the Fontan circulation. J Thorac Cardiovasc Surg 2006;132(5):1235-6.

27. Kelley JR, Mack GW, Fahey JT. Diminished venous vascular capacitance in patients with univentricular hearts after the Fontan operation. Am J Cardiol 1995;76(3):158-63.

28. Kiesewetter CH, Sheron N, Vettukattill JJ, Hacking N, Stedman B, Millward-Sadler H, et al. Hepatic changes in the failing Fontan circulation. Heart 2007;93(5):579-84.

29. Rodefeld MD, Boyd JH, Myers CD, LaLone BJ, Bezruczko AJ, Potter AW, et al. Cavopulmonary assist: circulatory support for the univentricular Fontan circulation. Ann Thorac Surg 2003;76(6):1911-6; discussion 1916.

30. Rodefeld MD, Boyd JH, Myers CD, Presson RG, Jr., Wagner WW, Jr., Brown JW. Cavopulmonary assist in the neonate: an alternative strategy for single-ventricle palliation. J Thorac Cardiovasc Surg 2004;127(3):705-11.

31. Frakes DH, Conrad CP, Healy TM, Monaco JW, Fogel M, Sharma S, et al. Application of an adaptive control grid interpolation technique to morphological vascular reconstruction. IEEE Trans Biomed Eng 2003;50(2):197-206.

32. Pekkan K, Kitajima HD, de Zelicourt D, Forbess JM, Parks WJ, Fogel MA, et al. Total cavopulmonary connection flow with functional left pulmonary artery stenosis: angioplasty and fenestration in vitro. Circulation 2005;112(21):3264-71.

33. Peskin CS, Tu C. Hemodynamics in congenital heart disease. Comput Biol Med 1986;16(5):331-59.

34. Migliavacca F, Pennati G, Dubini G, Fumero R, Pietrabissa R, Urcelay G, et al. Modeling of the Norwood circulation: effects of shunt size, vascular resistances, and heart rate. Am J Physiol Heart Circ Physiol 2001;280(5):H2076-86.

35. Palladino JL, L.C. R, Noordergraaf A. Human System Circulation Model Based on the Frank Mechansim. In: Ottesen JT, Danielson M, editors. Mathematical Modeling in Medicine: IOP Press; 2000. p. 29-40.

36. Sun Y, Beshara M, Lucariello RJ, Chiaramida SA. A comprehensive model for right-left heart interaction under the influence of pericardium and baroreflex. Am J Physiol 1997;272(3 Pt 2):H1499-515.

37. Milanesi O, Stellin G, Colan SD, Facchin P, Crepaz R, Biffanti R, et al. Systolic and diastolic performance late after the Fontan procedure for a single ventricle and comparison of those undergoing operation at <12 months of age and at >12 months of age. Am J Cardiol 2002;89(3):276-80.

38. Penny DJ, Redington AN. Diastolic ventricular function after the Fontan operation. Am J Cardiol 1992;69(9):974-5.

39. Minamisawa S, Nakazawa M, Momma K, Imai Y, Satomi G. Effect of aerobic training on exercise performance in patients after the Fontan operation. Am J Cardiol 2001;88(6):695-8.

40. Ohuchi H. Cardiopulmonary response to exercise in patients with the Fontan circulation. Cardiol Young 2005;15 Suppl 3:39-44.

41. Ohuchi H, Arakaki Y, Yagihara T, Kamiya T. Cardiorespiratory responses to exercise after repair of the univentricular heart. Int J Cardiol 1997;58(1):17-30.

42. Sanghavi DM, Flanagan M, Powell AJ, Curran T, Picard S, Rhodes J. Determinants of exercise function following univentricular versus biventricular repair for pulmonary atresia/intact ventricular septum. Am J Cardiol 2006;97(11):1638-43.

43. Bendien C, Bossina KK, Buurma AE, Gerding AM, Kuipers JR, Landsman ML, et al. Hemodynamic effects of dynamic exercise in children and adolescents with moderate-to-small ventricular septal defects. Circulation 1984;70(6):929-34.

44. Khairy P, Poirier N, Mercier LA. Univentricular heart. Circulation 2007;115(6):800-12.

45. de Zelicourt DA, Pekkan K, Parks J, Kanter K, Fogel M, Yoganathan AP. Flow study of an extracardiac connection with persistent left superior vena cava. J Thorac Cardiovasc Surg 2006;131(4):785-91.

46. Ensley AE, Lynch P, Chatzimavroudis GP, Lucas C, Sharma S, Yoganathan AP. Toward designing the optimal total cavopulmonary connection: an in vitro study. Ann Thorac Surg 1999;68(4):1384-90.

47. Ensley AE, Ramuzat A, Healy TM, Chatzimavroudis GP, Lucas C, Sharma S, et al. Fluid mechanic assessment of the total cavopulmonary connection using magnetic resonance phase velocity mapping and digital particle image velocimetry. Ann Biomed Eng 2000;28(10):1172-83.

48. Ryu K, Healy TM, Ensley AE, Sharma S, Lucas C, Yoganathan AP. Importance of accurate geometry in the study of the total cavopulmonary connection: computational simulations and in vitro experiments. Ann Biomed Eng 2001;29(10):844-53.

49. Sharma S, Goudy S, Walker P, Panchal S, Ensley A, Kanter K, et al. In vitro flow experiments for determination of optimal geometry of total cavopulmonary connection for surgical repair of children with functional single ventricle. J Am Coll Cardiol 1996;27(5):1264-9.

50. Soerensen DD, Pekkan K, de Zelicourt D, Sharma S, Kanter K, Fogel M, et al. Introduction of a new optimized total cavopulmonary connection. Ann Thorac Surg 2007;83(6):2182-90.

FIGURE LEGENDS

Figure 1: Three dimensional anatomic reconstructions of TCPC models used in this study. In total there are 6 intra-atrials (M01, M03, M04, M05, M14, M15), 9 extra-cardiacs (M02, M06, M07, M08, M09, M10, M12, M13, M16) and 1 IVC-MPA TCPC (M11).

Figure 2: The schematics describing the lumped parameter models used in the study. Shown on the left is the biventricular circulation (A), and to the right is the univentricular circulation (B). The abbreviations stand for: LA (Left Atrium), LV (Left Ventricle), SAB (Systemic Arterial Bed), SVB (Systemic Venous Bed), RA (Right Atrium), RV (Right Ventricle), PAB (Pulmonary Arterial Bed), PVB (Pulmonary Venous Bed), SA (Single Atrium), SV (Single Ventricle), TCPC (Total Cavopulmonary Connection).

Figure 3: TCPC resistance plotted as a function of cardiac index representing 16 geometries used in the study. These curves were used as inputs to the lumped parameter model. The maximum resistance curve corresponds to M16, while the minimum resistance model corresponds to M6. The mean resistance curve is the mean resistance at resting, moderate exercise, and severe exercise respectively.

Figure 4: Pressure and Flow waveforms at the aortic and pulmonary positions for the normal and single ventricle circulation respectively.

Figure 5: The impact of TCPC resistance on Cardiac Output (a), ESP (b), CVP (c), afterload (d), preload (e), and ventricular vascular coupling ratio (f) at resting conditions.

Figure 6: Pressure Volume loops at rest and exercise for the normal and single ventricle circulation with 0 resistance, low resistance, and high resistance.

Figure 7: The impact of increasing heart rate on cardiac output (a), end systolic pressure (b), central venous pressure (c), ventricular afterload (d), ventricular preload (e), vascular-

ventricular coupling (f), TCPC resistance (g), TCPC resistance/ PVR for the case of a normal biventricular circulation (rhombus), single ventricle scenarios with a low resistance TCPC (squares), mean resistance TCPC (circles), high resistance TCPCs (triangles).

Figure 8: Cardiac Index vs. Resistance for the 16 patients used in the study. The Cardiac Index was evaluated using MRI, and the resistance was evaluated using computational fluid dynamics.

TABLES

Table 1: Clinical data of patients used in the study

Model	CHD	Fontan Type	Age	Simulation conditions (L/Min)
M01	HLHS	IA	12	2,4,6
M02	DORV, PA	EC (BL)	9	2.5, 5, 7.5
M03	HLHS	IA	18	2.4, 4.8, 7.2
M04	TA	IA	10	2.9, 5.8, 8.7
M05	PA, HRHS	IA	15	2.75, 5.5, 8.25
M06	Heterotaxy, DC	EC (BL)	4	2.37, 4.72, 4.37
M07	DILV, TGA	EC	9	3.5, 7, 10.5
M08	DC, TA	EC	3	2.7, 3.7, 4.7
M09	TA	EC	7	3.03, 6.06, 9.09
M10	PA, HRHS	EC	8	3, 6, 9
M11	DORV, DC	IVC – MPA	7	3,4,5
M12	HLHS	EC	6	2,3,4
M13	HRHS	EC	5	3,4,5
M14	SV, DIAV	IA	3	2,3,4
M15	HLHS	IA	11	4,6,7
M16	HLHS	EC	6	2,3,4

Table 1: Diagnosis and simulation conditions of the models used in this study. CHD – Congenital Heart Disease, HLHS – Hypoplastic Left Heart Syndrome, IA – Intra-Atrial, DORV – Double Outlet Right Ventricle, Extra-Cardiac, BL – Bilateral SVC, DILV – Double Inlet Left

Ventricle, TGA – Transposition of Great Arteries, TA – Tricuspid Atresia, PA – Pulmonary Atresia, HRHS – Hypoplastic Right Heart Syndrome, SV – Single Ventricle, DIAV – Double Inlet Atrio-Ventricular Connection, MPA – Main Pulmonary Artery

Table 2: Parameters used in modeling the systemic and pulmonary circulation

Parameter	**Normal Ventricle**	**Single Ventricle**
C_{SVB} (mL/mmHg) [32]	1517	332.5
C_{SAB} (mL/mmHg)[32]	1.75	1.75
R_{SAB} (WU)*	17.2	17.2
R_{SVB} (WU) *	1.2	1.2
C_{PAB} (mL/mmHg)	4.12	4.12
C_{PVB} (mL/mmHg)	80	80
R_{PAB} (WU) *	1.7	1.7
R_{PVB} (WU) *	0.11	0.11

Table 2: Parameters used in the lumped parameter model. * Parameters extracted from patient data in the current study. WU is equivalent to mmHg/(L/Min).

Table 3: Parameters used for modeling the heart chambers

Parameter	Normal Heart	Single Ventricle Heart
CVD_{RA} (L/mmHg)	0.03	N/A
CVS_{RA} (L/mmHg)	0.0003	N/A
CVD_{RV} (L/mmHg)	0.0365	N/A
CVS_{RV} (L/mmHg)	0.0002	N/A
CVD_{LA} (L/mmHg)	0.01	0.01
CVS_{LA} (L/mmHg)	0.0003	0.0003
CVD_{LV} (L/mmHg)	0.0146	0.0146
CVS_{LV} (L/mmHg)	0.00003	0.00003
R_{Mi} (WU)	0.01	0.01
R_{Tr} (WU)	0.01	N/A
R_{Ao} (WU)	0.01	0.01
R_{Pu} (WU)	0.01	N/A

Table 3: Parameters used for describing the heart chambers in the mathematical model.

Table 4: Comparison of Predicted vs. Modeled data

Variable	Predicted	Observed	Average Percent Difference
CO (L/Min)	3.8	3.6 ± 1.7	5.2 %
$P_{systole}$ (mmHg)	115	114 ± 22	0.8 %
$P_{diastole}$ (mmHg)	73	63 ± 10	15.8 %
P_{SVB} (mmHg)	13	13.5 ± 3	0.6%

Table 4: Comparison of predicted and observed values of hemodynamic parameters from cardiac catheterization data acquired on 48 patients with a single ventricle physiology.

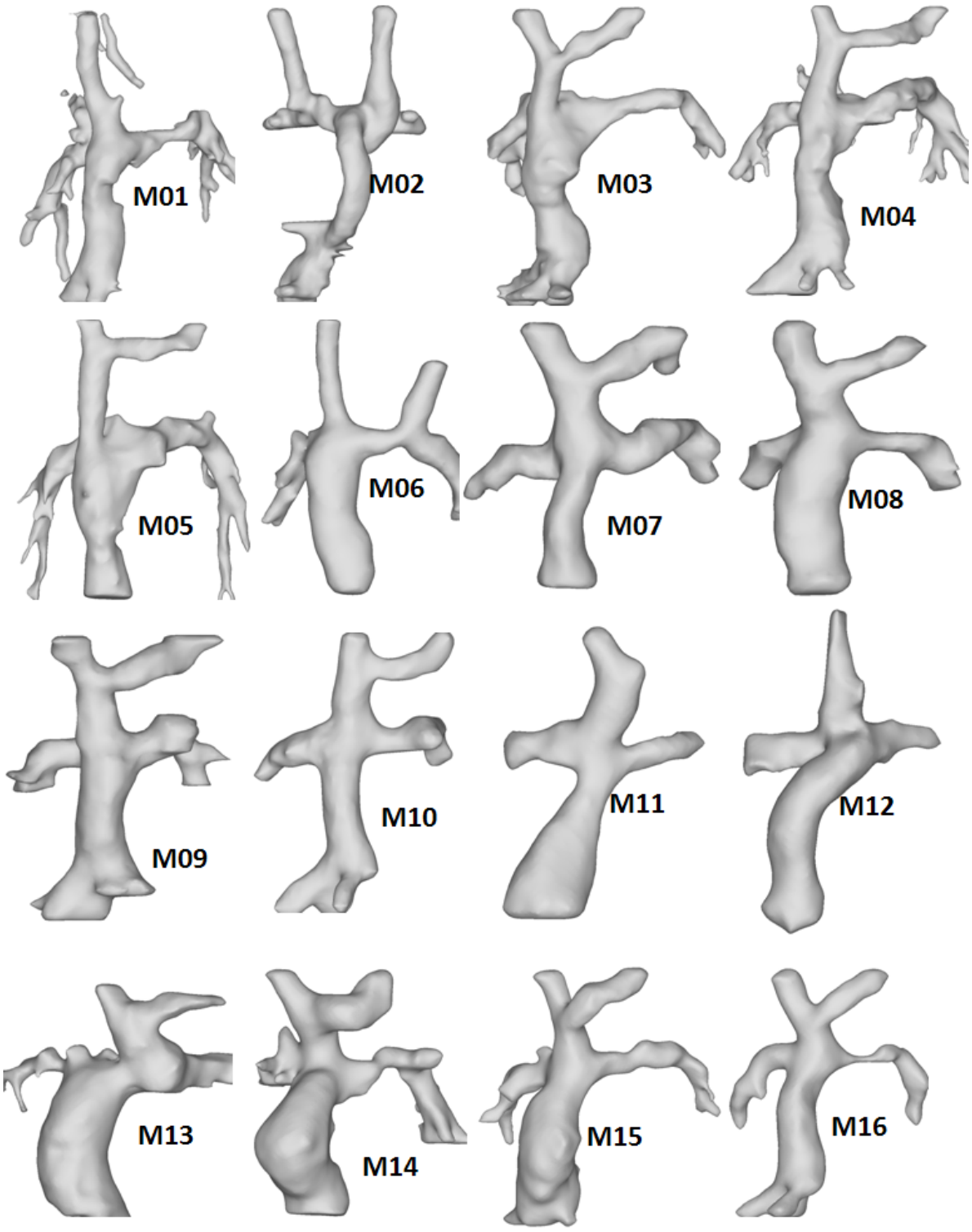
M01
M02
M03
M04
M05
M06
M07
M08
M09
M10
M11
M12
M13
M14
M15
M16

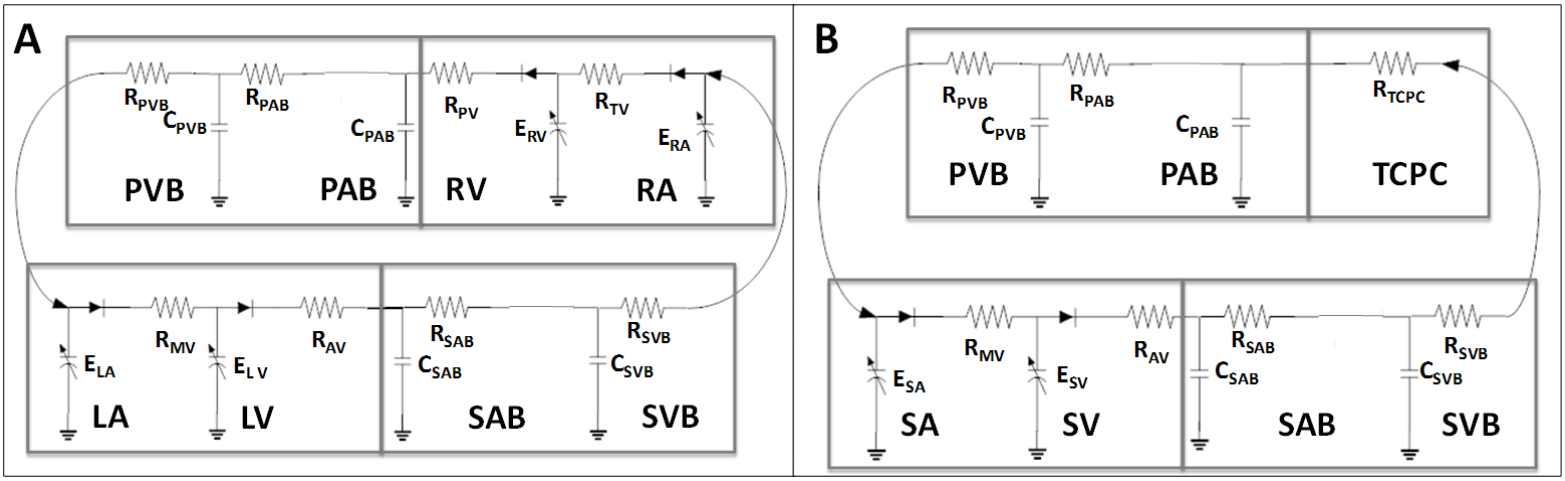
A
R_{PVB}
C_{PVB}
R_{PAB}
C_{PAB}
PVB
PAB
R_{PV}
E_{RV}
R_{TV}
E_{RA}
RV
RA
E_{LA}
R_{MV}
$E_{L V}$
R_{AV}
LA
LV
R_{SAB}
C_{SAB}
R_{SVB}
C_{SVB}
SAB
SVB
B
R_{PVB}
C_{PVB}
R_{PAB}
C_{PAB}
R_{TCPC}
PVB
PAB
TCPC
E_{SA}
R_{MV}
E_{SV}
R_{AV}
R_{SAB}
C_{SAB}
R_{SVB}
C_{SVB}
SA
SV
SAB
SVB

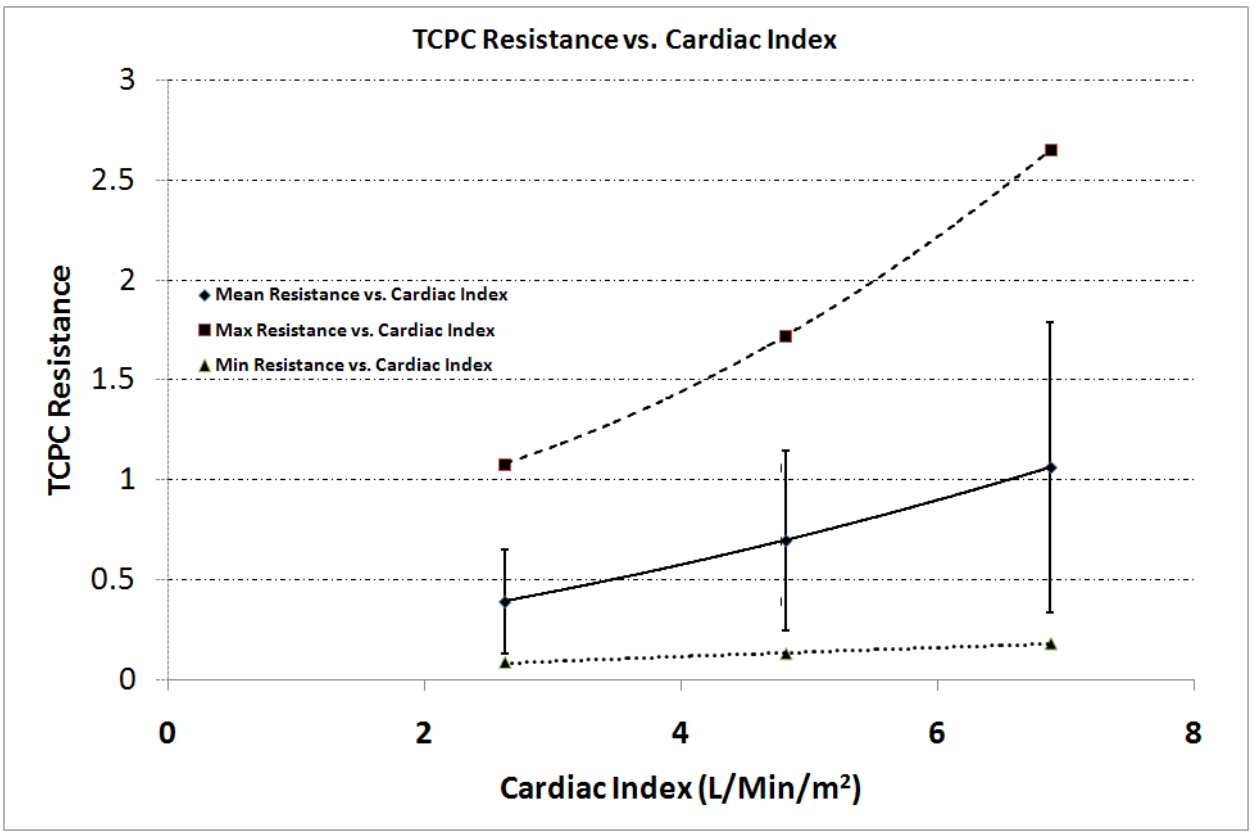
TCPC Resistance vs. Cardiac Index
TCPC Resistance
3
2.5
2
1.5
1
0.5
0
Mean Resistance vs. Cardiac Index
Max Resistance vs. Cardiac Index
Min Resistance vs. Cardiac Index
0
2
4
6
8
Cardiac Index (L/Min/m²)

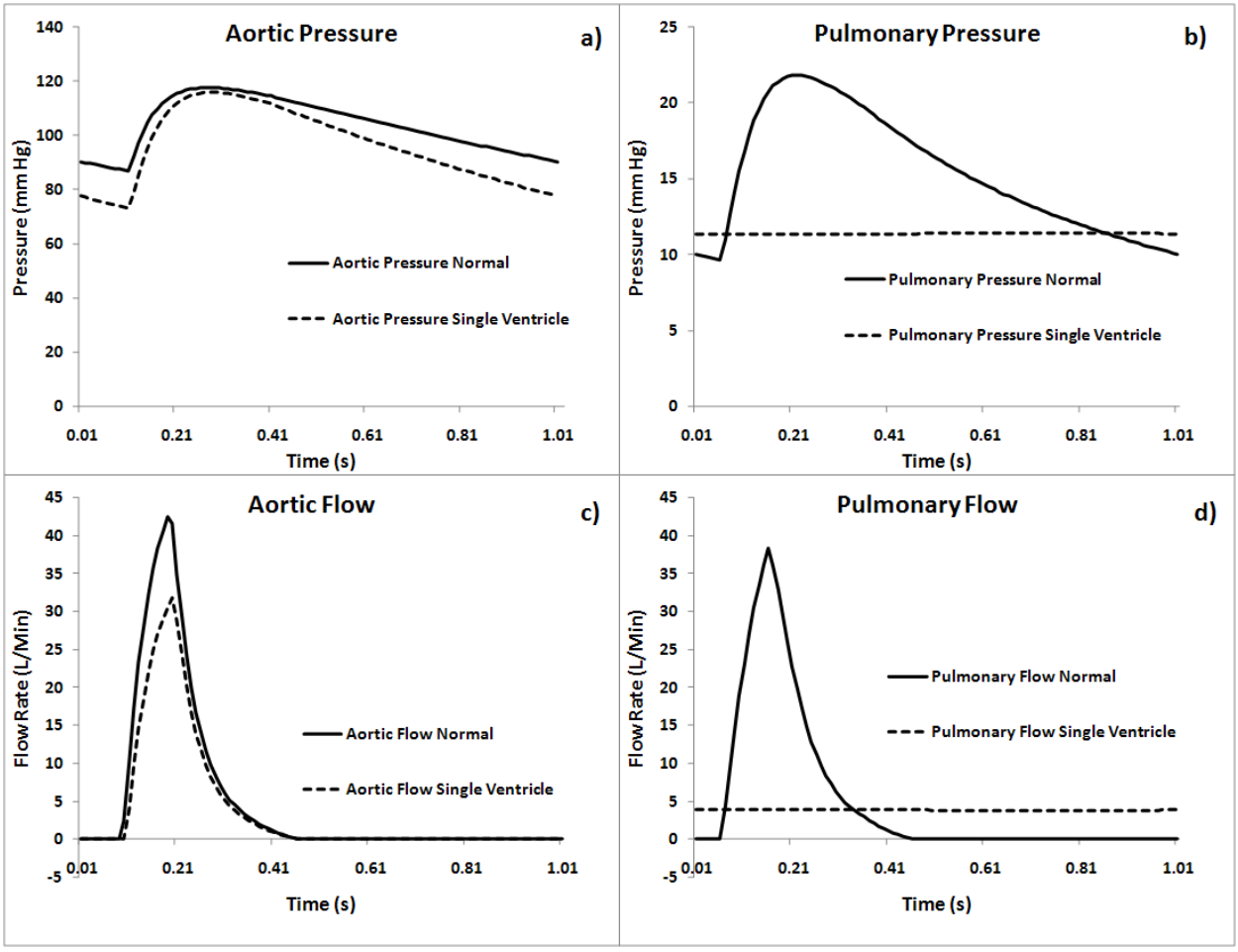
Aortic Pressure
a)
Pressure (mm Hg)
Time (s)
Aortic Pressure Normal
Aortic Pressure Single Ventricle
Pulmonary Pressure
b)
Pressure (mm Hg)
Time (s)
Pulmonary Pressure Normal
Pulmonary Pressure Single Ventricle
Aortic Flow
c)
Flow Rate (L/Min)
Time (s)
Aortic Flow Normal
Aortic Flow Single Ventricle
Pulmonary Flow
d)
Flow Rate (L/Min)
Time (s)
Pulmonary Flow Normal
Pulmonary Flow Single Ventricle

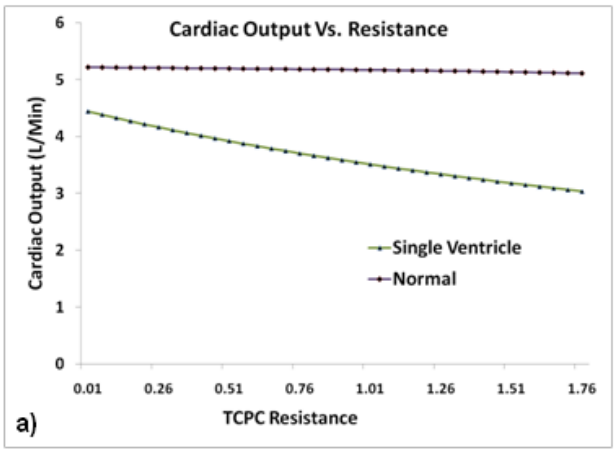
Cardiac Output Vs. Resistance
Cardiac Output (L/Min)
6
5
4
3
2
1
0
0.01
0.26
0.51
0.76
1.01
1.26
1.51
1.76
TCPC Resistance
Single Ventricle
Normal
a)

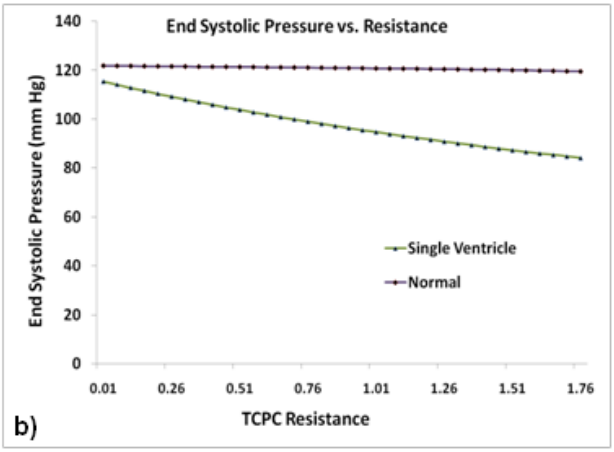
End Systolic Pressure vs. Resistance
End Systolic Pressure (mm Hg)
140
120
100
80
60
40
20
0
0.01
0.26
0.51
0.76
1.01
1.26
1.51
1.76
TCPC Resistance
Single Ventricle
Normal
b)

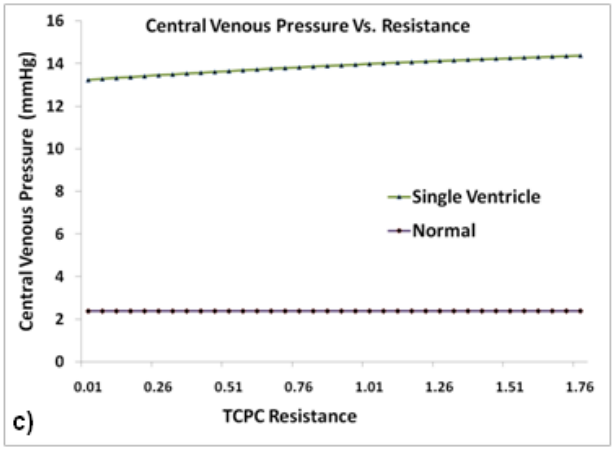
Central Venous Pressure Vs. Resistance
Central Venous Pressure (mmHg)
16
14
12
10
8
6
4
2
0
0.01
0.26
0.51
0.76
1.01
1.26
1.51
1.76
TCPC Resistance
Single Ventricle
Normal
c)

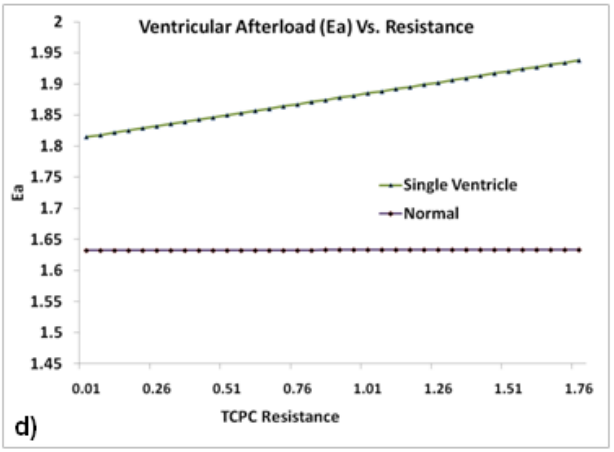
Ventricular Afterload (Ea) Vs. Resistance
Ea
2
1.95
1.9
1.85
1.8
1.75
1.7
1.65
1.6
1.55
1.5
1.45
0.01
0.26
0.51
0.76
1.01
1.26
1.51
1.76
TCPC Resistance
Single Ventricle
Normal
d)

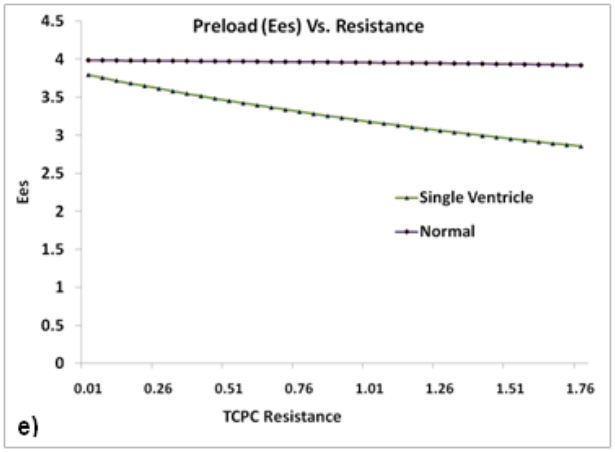
Preload (Ees) Vs. Resistance
Ees
4.5
4
3.5
3
2.5
2
1.5
1
0.5
0
0.01
0.26
0.51
0.76
1.01
1.26
1.51
1.76
TCPC Resistance
Single Ventricle
Normal
e)

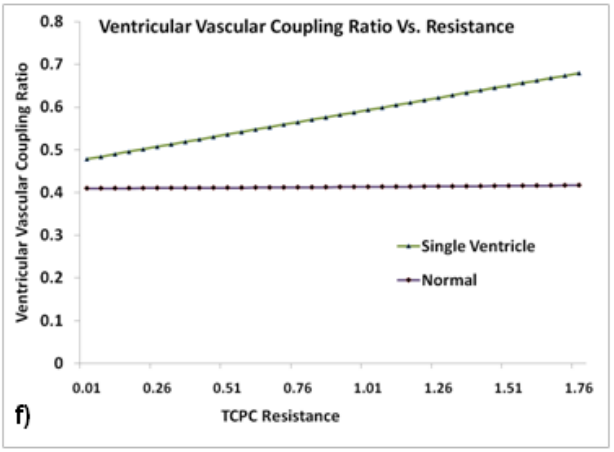
Ventricular Vascular Coupling Ratio Vs. Resistance
Ventricular Vascular Coupling Ratio
0.8
0.7
0.6
0.5
0.4
0.3
0.2
0.1
0
0.01
0.26
0.51
0.76
1.01
1.26
1.51
1.76
TCPC Resistance
Single Ventricle
Normal
f)

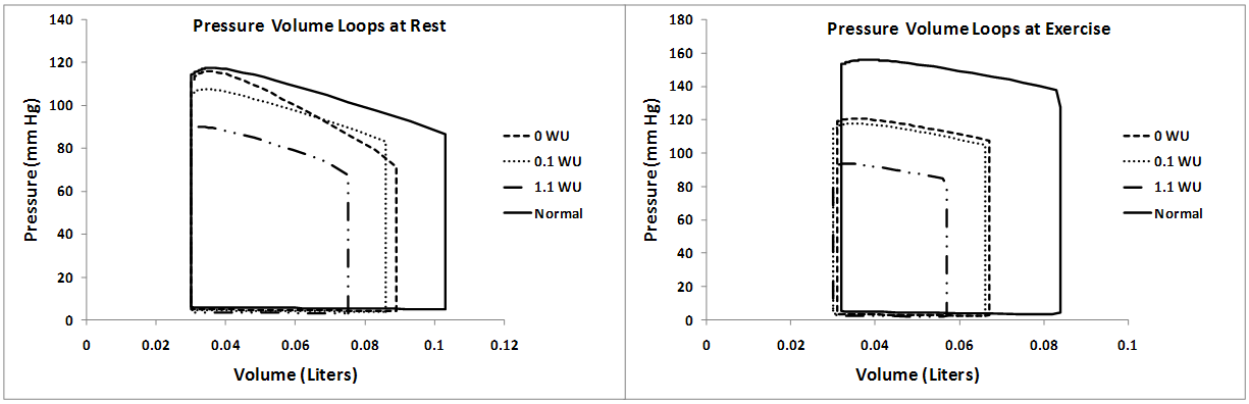
Pressure Volume Loops at Rest
Pressure (mm Hg)
Volume (Liters)
0 WU
0.1 WU
1.1 WU
Normal
Pressure Volume Loops at Exercise
Pressure (mm Hg)
Volume (Liters)
0 WU
0.1 WU
1.1 WU
Normal

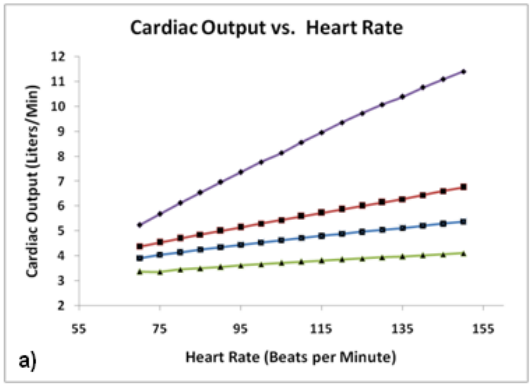
Cardiac Output vs. Heart Rate
Cardiac Output (Liters/Min)
12
11
10
9
8
7
6
5
4
3
2
55
75
95
115
135
155
Heart Rate (Beats per Minute)
a)

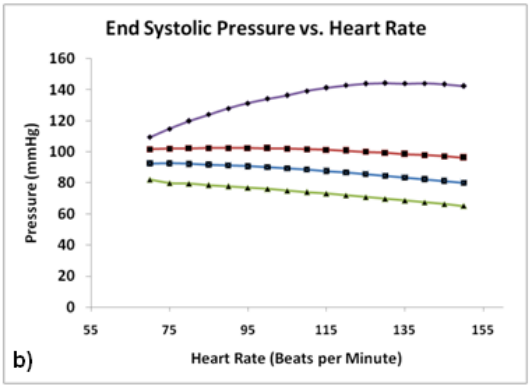
End Systolic Pressure vs. Heart Rate
Pressure (mmHg)
160
140
120
100
80
60
40
20
0
55
75
95
115
135
155
Heart Rate (Beats per Minute)
b)

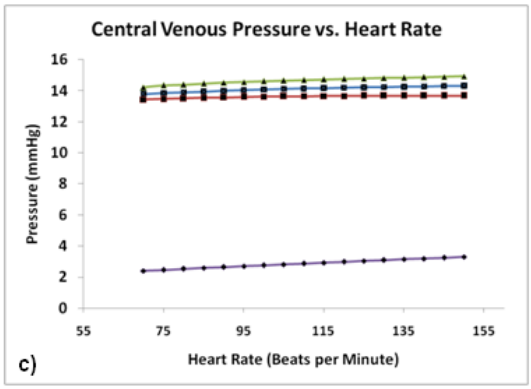
Central Venous Pressure vs. Heart Rate
Pressure (mmHg)
16
14
12
10
8
6
4
2
0
55
75
95
115
135
155
Heart Rate (Beats per Minute)
c)

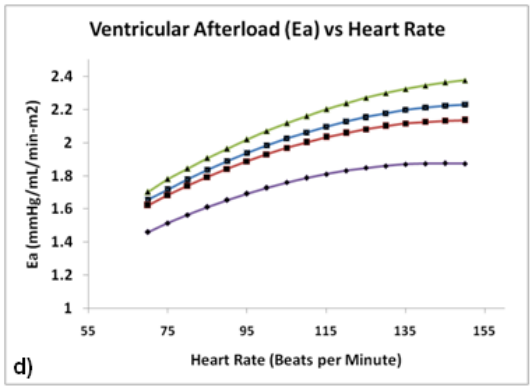
Ventricular Afterload (Ea) vs Heart Rate
Ea (mmHg/mL/min-m2)
2.4
2.2
2
1.8
1.6
1.4
1.2
1
55
75
95
115
135
155
Heart Rate (Beats per Minute)
d)

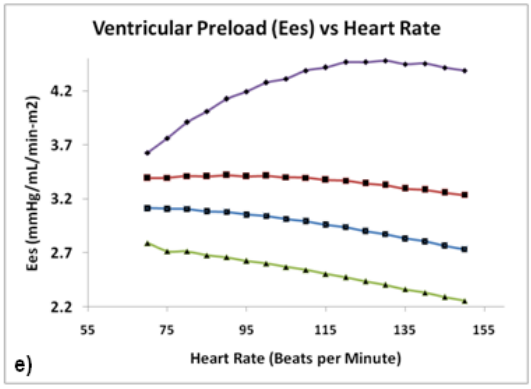
Ventricular Preload (Ees) vs Heart Rate
Ees (mmHg/mL/min-m2)
4.2
3.7
3.2
2.7
2.2
55
75
95
115
135
155
Heart Rate (Beats per Minute)
e)

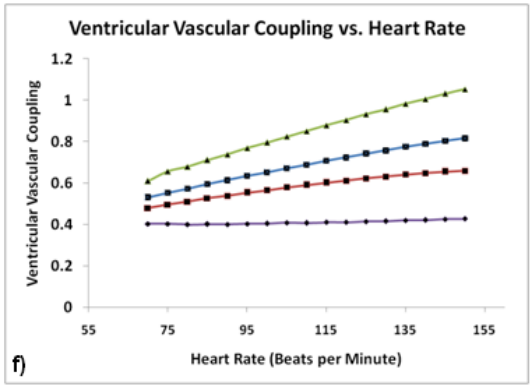
Ventricular Vascular Coupling vs. Heart Rate
Ventricular Vascular Coupling
1.2
1
0.8
0.6
0.4
0.2
0
55
75
95
115
135
155
Heart Rate (Beats per Minute)
f)

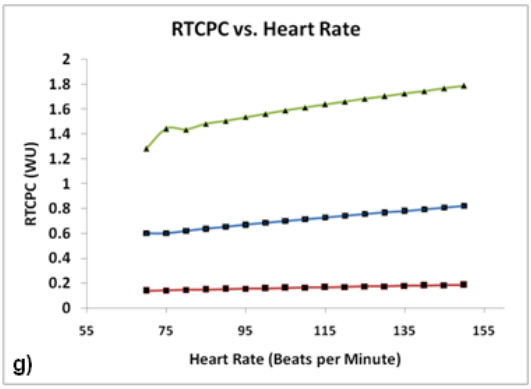
RTCPC vs. Heart Rate
RTCPC (WU)
2
1.8
1.6
1.4
1.2
1
0.8
0.6
0.4
0.2
0
55
75
95
115
135
155
Heart Rate (Beats per Minute)
g)

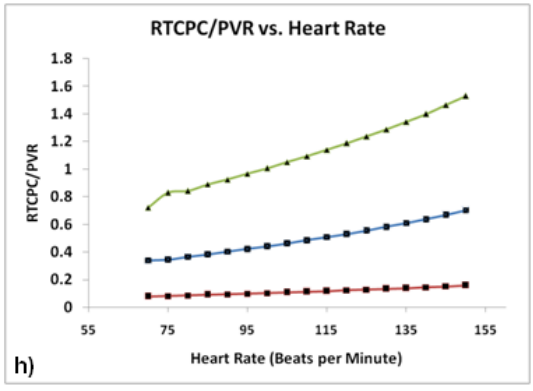
RTCPC/PVR vs. Heart Rate
RTCPC/PVR
1.8
1.6
1.4
1.2
1
0.8
0.6
0.4
0.2
0
55
75
95
115
135
155
Heart Rate (Beats per Minute)
h)

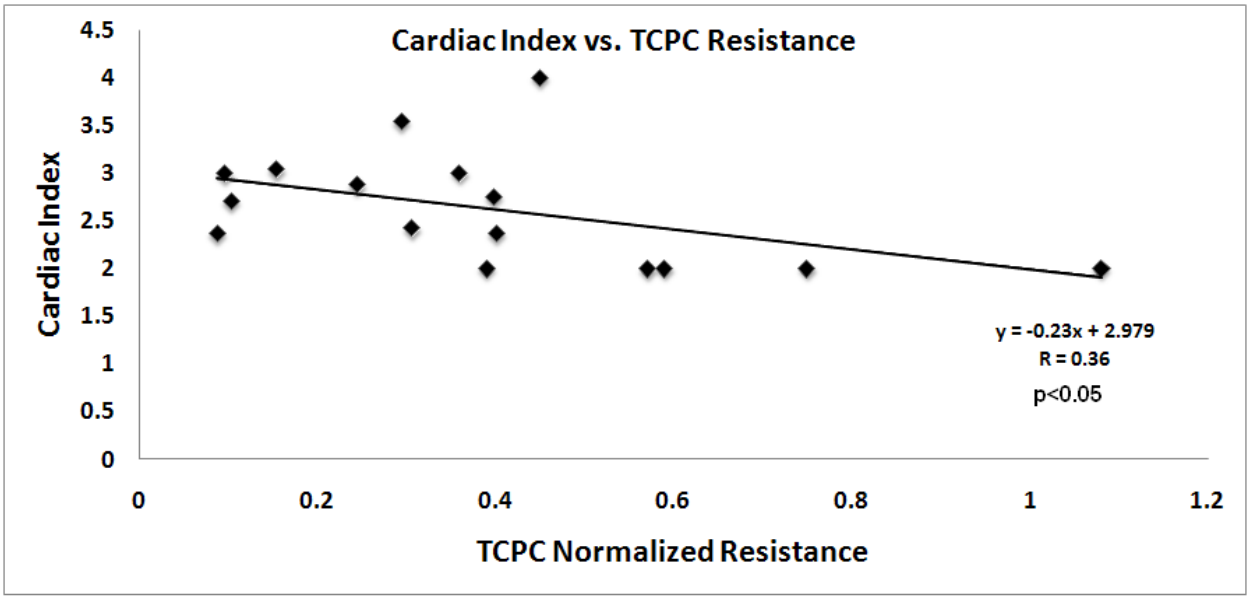
Cardiac Index vs. TCPC Resistance
Cardiac Index
TCPC Normalized Resistance
y = -0.23x + 2.979
R = 0.36
p<0.05
4.5
4
3.5
3
2.5
2
1.5
1
0.5
0
0
0.2
0.4
0.6
0.8
1
1.2